

SUPPORTING INFORMATION

Anion-Induced Morphological Regulation of Cupric Oxide Nanostructures and Their Application as Co-catalyst for Solar Water Splitting

Truong-Giang Vo¹, Shu-Ju Chang¹, Chia-Ying Chiang^{1}*

*¹ Department of Chemical Engineering, National Taiwan University of Science and Technology,
Taipei-106, Taiwan*

*Corresponding Authors:

Prof. **Chia-Ying Chiang**

Phone: +886-2-2737-6641

Fax: +886-2-2737-6641

E-mail: cychiang@mail.ntust.edu.tw

Reagents and materials

All chemicals used in this study had reagent-grade purity. Copper (II) nitrate, sodium nitrate, *p*-benzoquinone, sodium hydroxide was purchased from Acros Organics. All solutions were prepared using deionized water. Fluorine doped tin oxide (FTO) coated glass plate (15 Ω /sq) of thickness 2.2 mm was used as the substrate.

Fabrication of BiVO₄ Photoelectrodes

In a typical deposition, 32 mM Bi(NO₃)₃ and 48 mM vanadium (IV)-oxyacetylacetonate was dissolved in a mixture of acetylacetone and acetic acid (8.25:1, v/v). The dark green solution was sonicated for 20 min, then was filtered with 0.22 μ m nylon filters before being dispensed onto fluorine-doped tin oxide (FTO) glass. The spin coating of the precursor solution onto FTO was conducted with the speed of 2500 rpm for 20 s for a single layer coating, and the calcination in the air was followed. For the first three layers, the sample was annealed at 500 °C for 10 min in a muffle furnace. From layer 4 to 6, the sample was maintained at 500 °C for 2 h. After the last spin-coating cycle, the substrate was annealed for 4 h at 500 °C to ensure a better crystallinity of BiVO₄. During the period of temperature elevation to 500 °C, the heating rate was set at 3 °C/min.

It can be found that the characteristic peaks of Cu-LHS/S has shifted to lower 2θ values compared Cu-LHS/N, revealing the increasing in crystal layer spacing of Cu-LHS/S in order to accommodate the SO_4^{2-} which is bigger in size

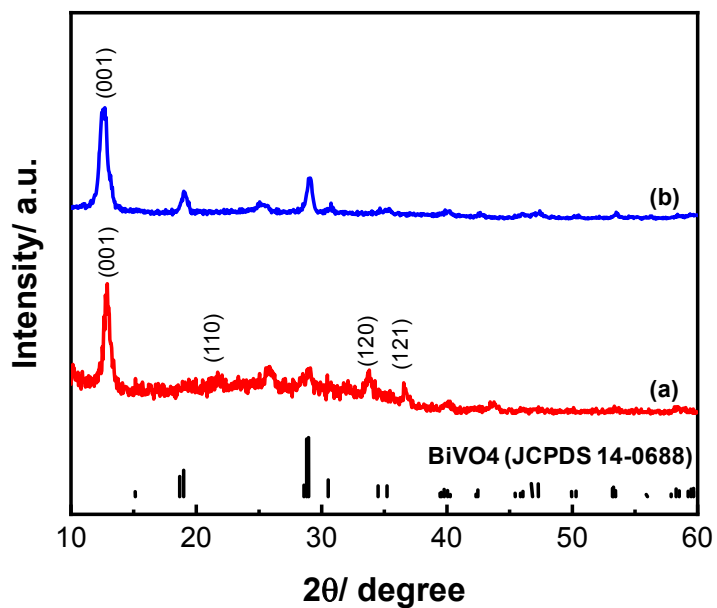


Figure S1 XRD patterns of as-deposited (a) Cu-LHS/N corresponding to $(\text{Cu}_2\text{NO}_3(\text{OH})_3)$, (b) Cu-LHS/S corresponding to $(\text{Cu}_4\text{SO}_4(\text{OH})_6)$.

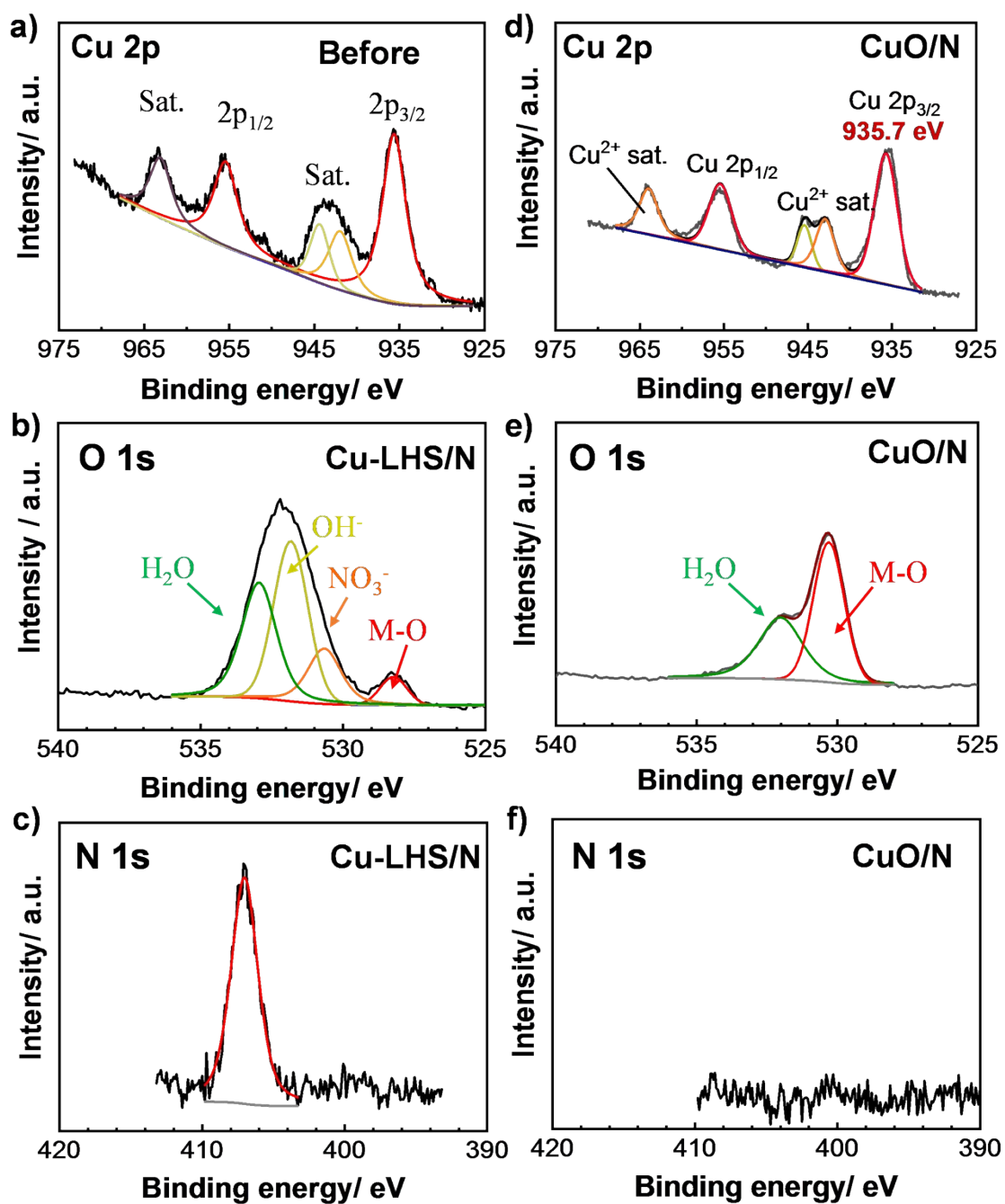


Figure S2 HR-XPS spectra of Cu 2p, O 1s, N 1s for Cu-LHS/N (a-c) and CuO-N (d-f).

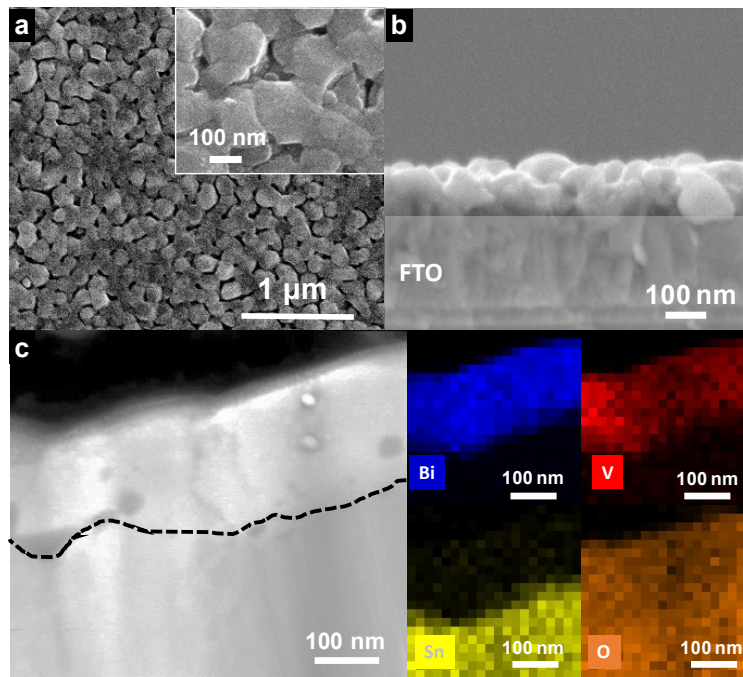


Figure S3 (a) Top-view, (b) side-view of BVO thin film substrate and (c) STEM-HAADF image and elemental maps images of Bi (blue), V (red), Sn (yellow) and O (orange).

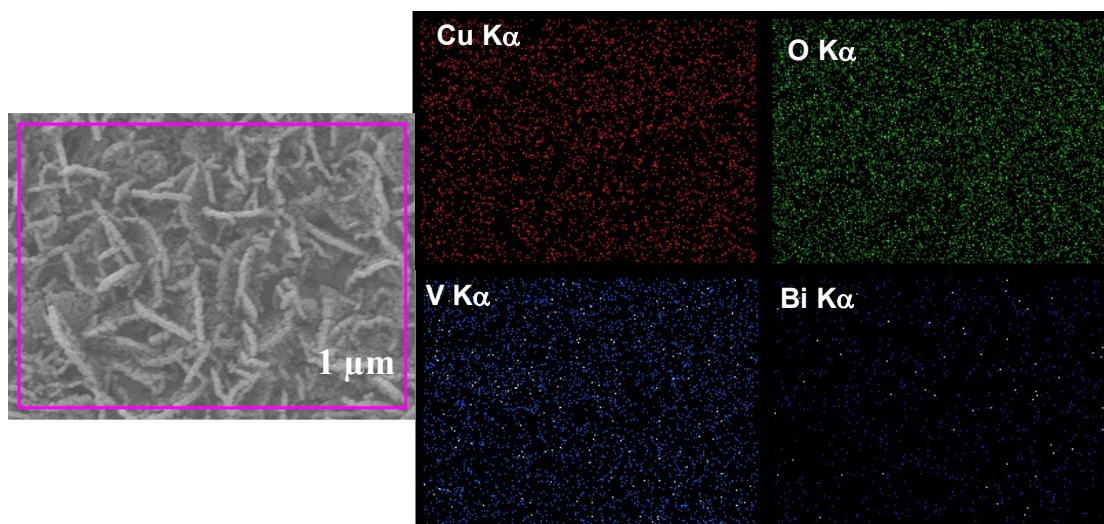


Figure S4 Electron images and elemental maps images of Bi (violet), V (blue), Cu (red) and O (green) for BVO/CuO-N sample.

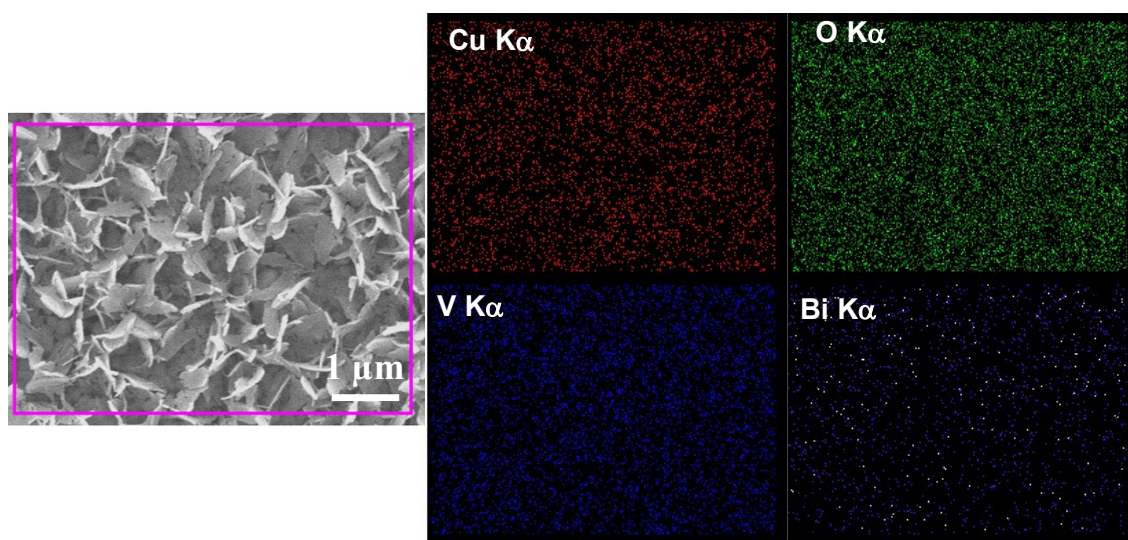


Figure S5 Electron images and elemental maps images of Bi (violet), V (blue), Cu (red) and O (green) for BVO/CuO-S sample.

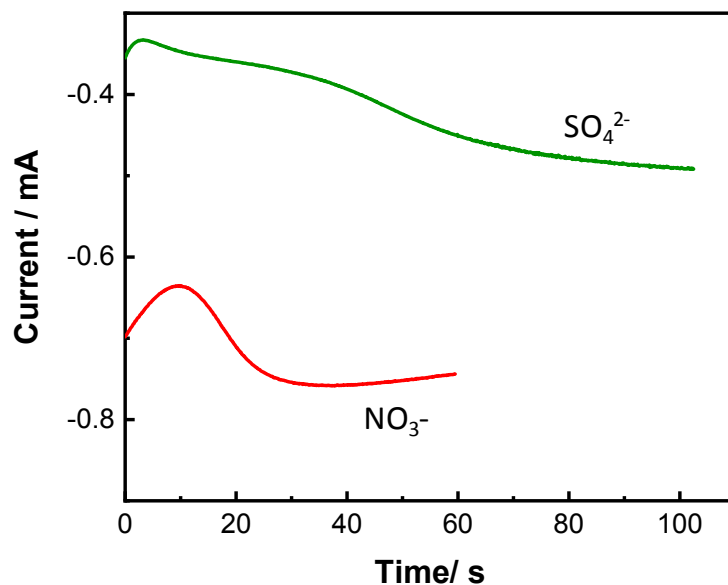


Figure S6 Change in current density during potentiostatic electrodeposition at 0 V vs. Ag/AgCl from solutions containing sulfate or nitrate ions as counter anions

The electrochemical behaviors of the as-made CuO/FTO for the OER are evaluated in 0.1M NaOH solution, of which the detailed results are demonstrated Figure S7. Obviously, both CuO-S and CuO-N samples did show OER catalytic activity in basic solution although its performance is much less inferior to other reports where highly porous and conductive substrates, e.g. Ni foam, was used.

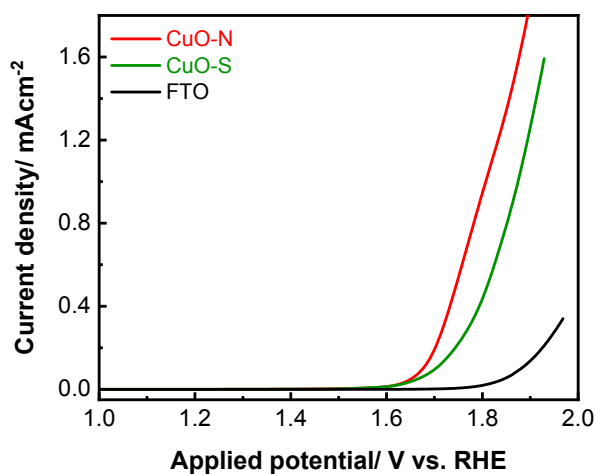


Figure S7 LSV of CuO-N and CuO-S for oxygen evolution reaction in 0.1M NaOH (pH 13)

The electrochemical active surface area of the catalysts was estimated based on the double-layer capacitance (C_{dl}) of the catalysts. Cyclic voltammetry (CV) in a potential window where no Faradaic processes took place was used to test the catalysts under different scan rates. The C_{dl} can be estimated by the slope of a linear fitting for the current density vs. scan rate plot.

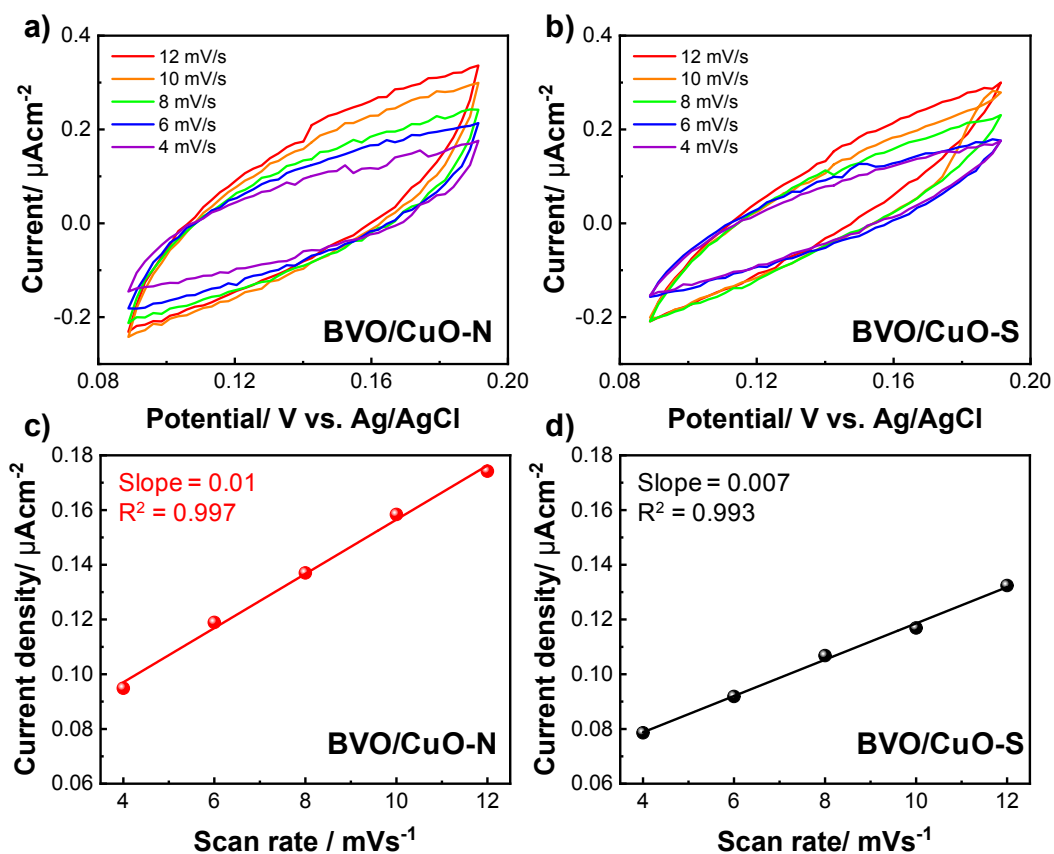


Figure S8 (a, b) CV scans near the open circuit potential (OCP) and (c, d) current densities at 0.14 V vs. RHE plotted against scan rate for BVO/CuO-N and BVO/CuO-S.

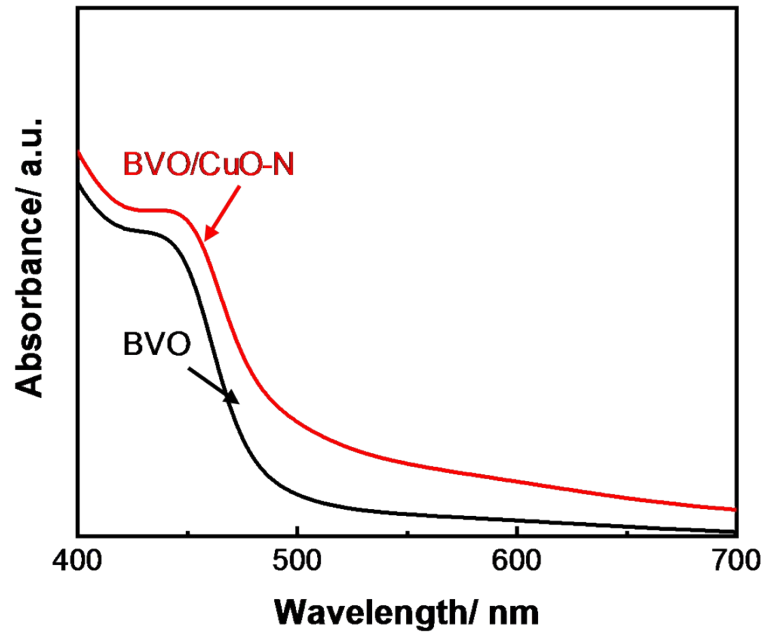


Figure S9 UV-Vis absorption of BVO and BVO/CuO-N photoanode.

In order to investigate the recombination kinetics of photogenerated charge carriers, time-resolved photoluminescence (TRPL) measurements were performed on bare BVO and BVO/CuO-N with 405 nm laser excitation, and the emission intensity was monitored at 530 nm. The PL decay profiles are fitted using a biexponential decay function expressed as follows^{1,2}:

$$I(t) = A_1 \exp(t/\tau_1) + A_2 \exp(t/\tau_2)$$

The average excited state lifetime can be calculated by using the following relationship^{3,4}

$$\tau_{avg} = \frac{\sum_{i=1}^2 A_i \tau_i^2}{\sum_{i=1}^2 A_i \tau_i}$$

Where τ_i is the lifetime of individual component and A_i is the corresponding amplitude.

For both BVO and BVO/CuO-N, the TRPL decay curves could be fit with a biexponential decay pattern, where the fast component (τ_1) most likely corresponds to the electron trapping at defects and the slow one (τ_2) is owing to the electron-hole recombination^{2,5}. The details of the time constants (τ_i) and amplitudes (A_i) of bare BVO and BVO/CuO-N are tabulated in **Table S1**.

Table S1 Results of time-resolved PL data of the BVO and BVO/CuO-N

Sample	τ_1 (ps)	A_1	τ_2 (ps)	A_2	τ_{avg} (ps)
BVO	84.5	0.977	783.7	0.023	209.8
BVO/CuO	67.1	0.987	817.7	0.013	170.9

- 1 S. Nayak, L. Mohapatra and K. Parida, *J. Mater. Chem. A*, 2015, **3**, 18622–18635.
- 2 J. Nong, G. Lan, W. Jin, P. Luo, C. Guo, X. Tang, Z. Zang and W. Wei, *J. Mater. Chem. C*, 2019, **7**, 9830–9839.
- 3 Z. Lin, C. Du, B. Yan and G. Yang, *Catal. Sci. Technol.*, 2019, **9**, 5582–5592.
- 4 T. Xie, Y. Liu, H. Wang and Z. Wu, *Sci. Rep.*, 2019, **9**, 7551.
- 5 K. Zhang, B. Jin, C. Park, Y. Cho, X. Song, X. Shi, S. Zhang, W. Kim, H. Zeng and J. H. Park, *Nat. Commun.*, 2019, **10**, 2001.

Flate-band estimation by Mott-Schottky measurement

The conduction band (CB) of an n-type semiconductor or the valence band (VB) of a p-type semiconductor can also be measured by PEC through Mott-Schottky plot.

For an n-type semiconductor:

$$\frac{1}{C^2} = \frac{2}{\epsilon\epsilon_0 A^2 N_D} \left(V - V_{FB} - \frac{k_B T}{e} \right)$$

whereas for a p-type semiconductor:

$$\frac{1}{C^2} = \frac{2}{\epsilon\epsilon_0 A^2 N_A} \left(V_{FB} - V - \frac{k_B T}{e} \right)$$

where C (F) is the space-charge capacitance; A (cm^2) is the active geometric area; N_D (cm^{-3}) is the donor density; e is the electronic charge; ϵ is the dielectric constant of the semiconductor; ϵ_0 is the vacuum permittivity ($\epsilon_0 = 8.854 \times 10^{-12}$ F m^{-1}); V is the applied potential; V_{FB} (V vs. RHE) is the flat-band potential; k_B is the Boltzmann constant ($k_B = 1.381 \times 10^{-23}$ J K^{-1}); T is the temperature ($T = 298$ K). N_D and N_A are the number of donors and acceptors for n-type and p-type semiconductors, respectively.

The flat band potential (V_{fb}) of electrode is represented by the x-intercept of a plot of $1/C^2$ against V according to the Mott-Schottky equation. Also, it is generally accepted that higher slope of graph (C^{-2} vs. V) means lower electron donor densities, which is given by equation:

$$\text{slope of graph } (C^{-2} \text{ vs. } V) = 2e\epsilon\epsilon_0 A N_d$$

Calculation of the Faradaic efficiency

The dashed lines in the plot below is gas concentration predicted from the photocurrent assuming 100% faradaic efficiency, and the points are experimentally measured gas concentration. The faradaic efficiency was calculated by dividing the experimentally measured amount by the amount of O₂ predicted from the photocurrent.

To be specific, under a constant oxidation current (I) within a certain time (t), the experimentally produced O₂ amount can be detected by gas chromatography. Assuming that the production of one O₂ molecule needs to consume four electrons, the corresponding theoretically produced O₂ amount can be obtained according to the following equation: $n_{theoretical} = (It)/4F$. Therefore, the Faradaic efficiency can be calculated as follows:

$$\text{Faradaic efficiency} = (n_{O_2\text{experimental}})/n_{O_2\text{theoretical}} = 4Fn_{O_2}/(It).$$

with I being the current, z being the number of transferred charges (i.e. $z = 4$ for water oxidation) and the Faraday constant (F) = 96485 C/mol.

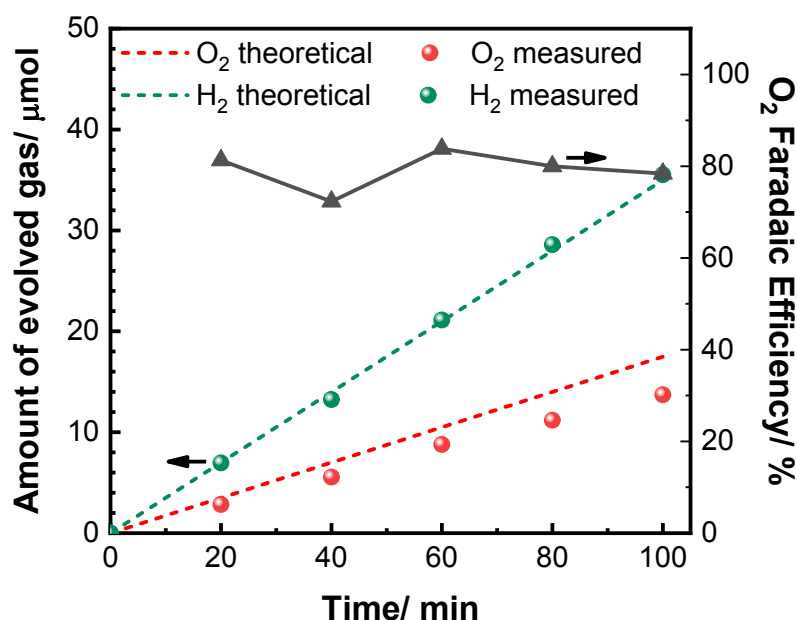


Figure S10 Amount of evolved O₂ (red dot) and H₂ (blue triangle) produced from water oxidation for bare BVO photoanode (1.5 cm × 1.5 cm) under constant current of 0.5 mA/cm² in borate buffer. Red and blue dashed lines are the theoretical amount of O₂ and H₂, respectively.

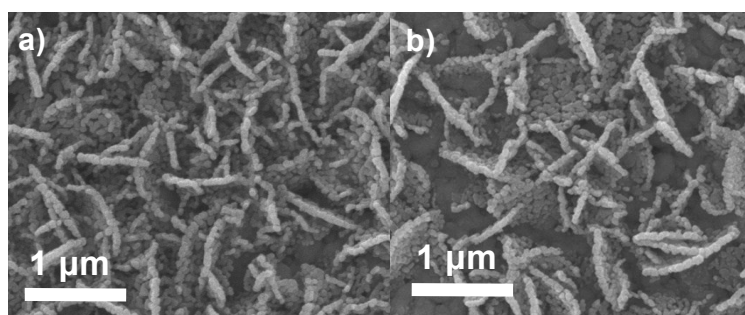


Figure S11 SEM images of BVO/CuO-N before and after OER.

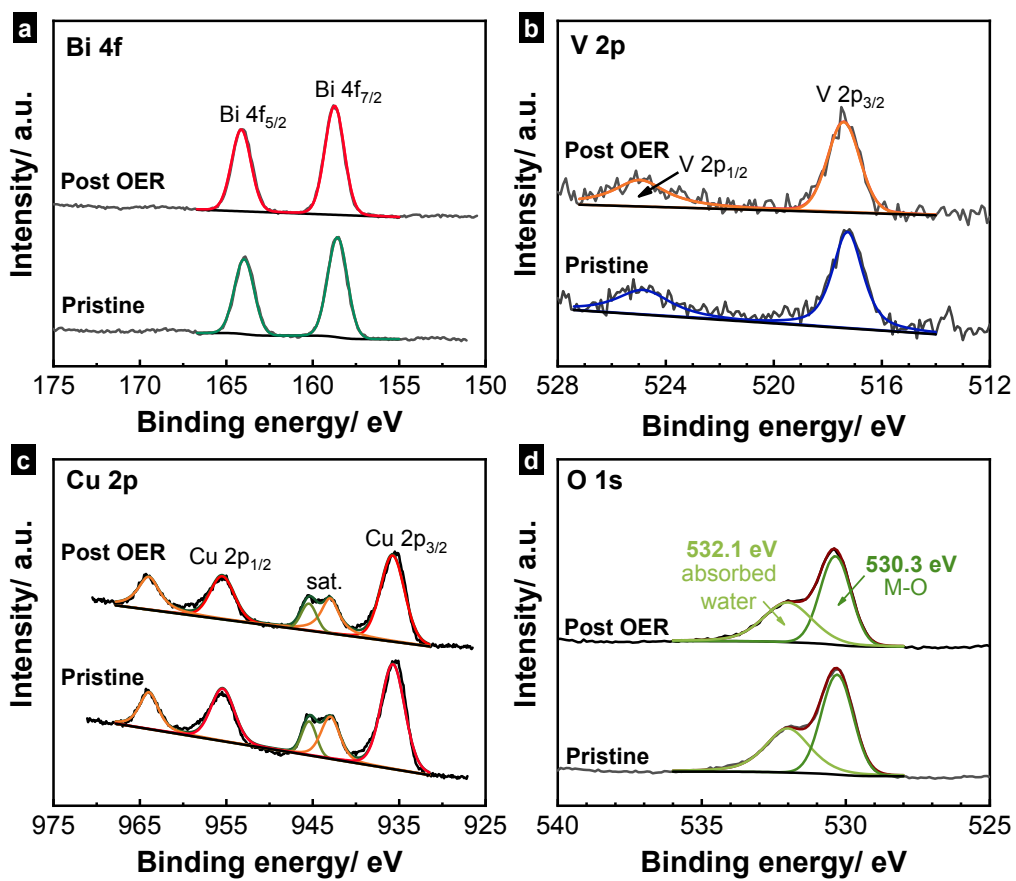


Figure S12 High-resolution XPS of Bi 4f (a), V 2p (b), Cu 2p (c) and O 1s (d) in BVO/CuO-N before and after OER.